Journal of Polymer Science

WILEY

JOURNAL OF POLYMER SCIENCE

RESEARCH ARTICLE OPEN ACCESS

Polybutadiene Modification of Brown Grease-Sulfur Materials

Bárbara G. S. Guinati[1] | Andrew G. Tennyson[1,2] | Ashlyn D. Smith[1] | Rhett C. Smith[1]

[1]Department of Chemistry, Clemson University, Clemson, South Carolina, USA | [2]Department of Materials Science and Engineering, Clemson University, Clemson, South Carolina, USA

Correspondence: Ashlyn D. Smith (ashlynd@clemson.edu) | Rhett C. Smith (rhett@clemson.edu)

Received: 1 May 2025 | **Revised:** 30 July 2025 | **Accepted:** 5 August 2025

Funding: This work was supported by Division of Chemistry, CHE-2203669.

Keywords: brown grease | polybutadiene | sulfur | triglyceride

ABSTRACT

High sulfur-content materials (HSMs) prepared via inverse vulcanization are attractive for a range of sustainable material applications, particularly when synthesized from waste-derived feedstocks such as brown grease (BG). Two BG-based composites, **SunBG$_{90}$** and **aBG$_{90}$**, were prepared using elemental sulfur and either native or allylated brown grease, respectively. This study explores the effect of reinforcing these sulfur-rich networks with low loadings (0.5–2 wt. %) of high *cis*-1,4-content liquid polybutadiene (PBD). Incorporation of PBD resulted in significant increases in storage modulus, with a near-linear relationship between PBD content and stiffness enhancement for both material types. At −60°C, storage modulus increased more than fivefold for **aBG$_{90}$** and more than tripled for **SunBG$_{90}$**. In contrast, flexural strength and flexural modulus exhibited non-linear responses, with diminishing or reversed gains at higher PBD loadings, suggesting limits to rubber domain compatibility and dispersion. Thermal analysis confirmed high decomposition temperatures (212°C–226°C) and stable glass transitions, indicating thermal robustness of the reinforced networks. Compared with previous studies requiring higher PBD loadings, these results demonstrate that BG-based HSMs can be effectively reinforced at low additive levels, offering mechanically robust, low-cost, and renewable alternatives for structural applications.

1 | Introduction

High sulfur-content materials (HSMs) prepared by inverse vulcanization [1, 2] have emerged as promising materials for a wide range of applications requiring specific optical [3], electrochemical [4–6], absorbent [7, 8], adhesive [9–12], or mechanical properties [13–16]. Traditional vulcanization [17, 18] transforms unsaturated polymers (e.g., natural rubber) into crosslinked materials using elemental sulfur; in contrast, inverse vulcanization (Scheme 1A) uses elemental sulfur as both the major component (> 50 wt. % sulfur) and the crosslinking agent [9, 19–22]. In doing so, sulfur, a by-product of the petroleum refining industry that is routinely stockpiled in landfills or discarded [23], becomes a value-added feedstock, converted into high-performance materials [24, 25]. Furthermore, the thermal reversibility of S–S bond formation in HSM oligo- or polysulfur crosslinkers facilitates facile thermal processing and recycling of many HSMs [13, 15, 26–44]. Over the past decade, diverse organic comonomers have been explored for inverse vulcanization, ranging from small-molecule olefins such as dicyclopentadiene or divinylbenzene to bio-derived resins from fats, plant oils, and lignocellulosic sources [26, 45–48].

Brown grease (BG) has garnered attention as one such sustainable comonomer for inverse vulcanization [47, 49–53]. Generated in large volumes during food production, BG typically contains high levels of free fatty acids and other lipids and contaminants, making it inappropriate for human or

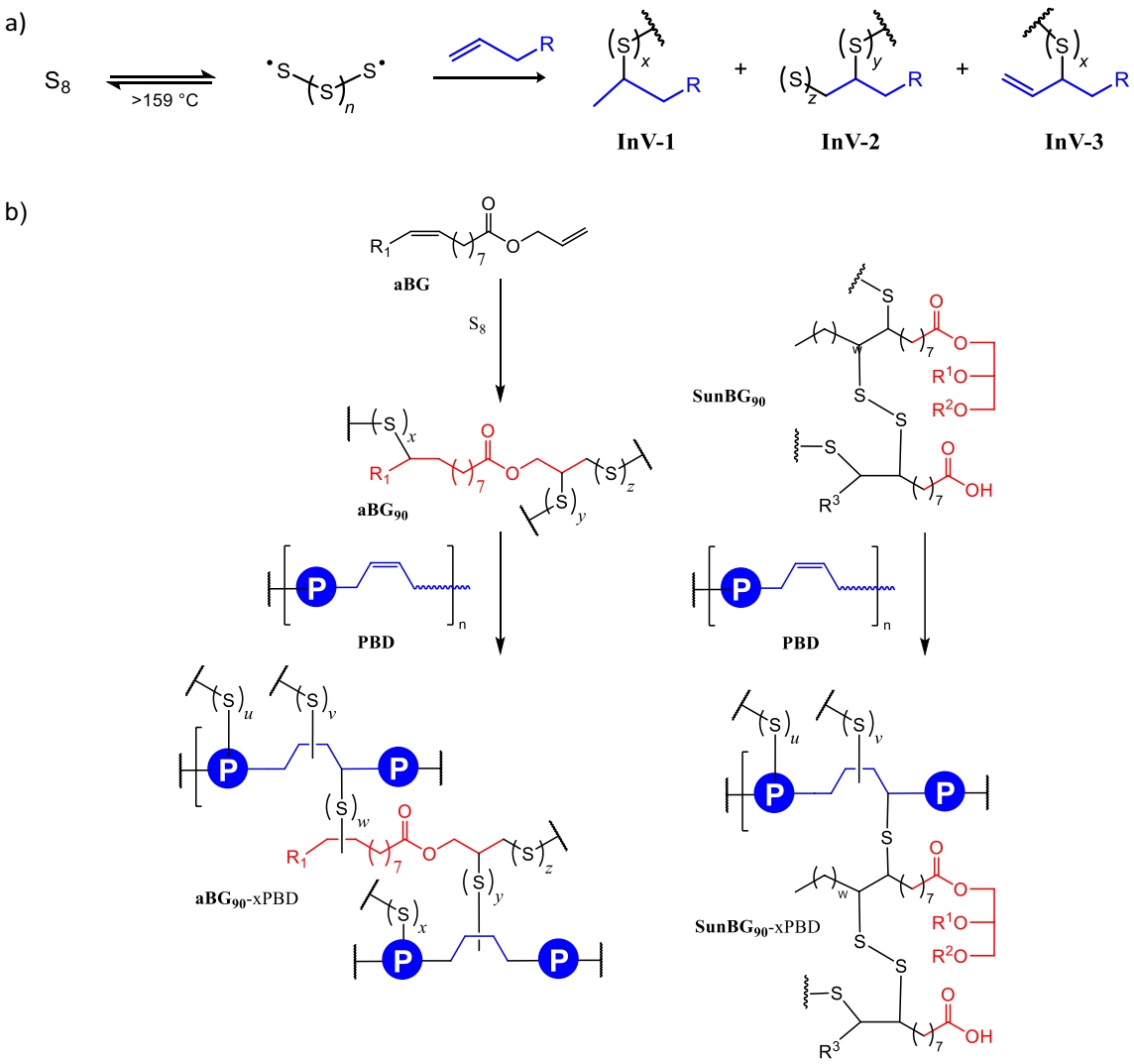

SCHEME 1 | (a) General scheme for inverse vulcanization and (b) incorporation of PBD to reinforce **aBG$_{90}$** and **SunBG$_{90}$**. Here, one representative chain of a brown grease-derived fatty acid or glyceride chain is shown, and P represents PBD segments that contain *cis*-1,4-, *trans*-1,4-, and 1,2-vinyl linkages, which may also undergo crosslinking at the olefins or allylic sites.

animal consumption. The most well-studied BG-derived HSM is **SunBG$_{90}$** (90 wt. % elemental sulfur, 5 wt. % brown grease, and 5 wt. % sunflower oil) [47]. The scalability of **SunBG$_{90}$** to multi-kilogram batches suitable for standardized testing has been demonstrated [52]. The findings from multiple studies underscore the viability of **SunBG$_{90}$** as a sustainable alternative to ordinary Portland Cement (OPC). Compared with OPC, **SunBG$_{90}$** exhibits 84% lower water absorption, significantly enhancing its resistance to freeze–thaw cycles and moisture-induced degradation. **SunBG$_{90}$** has superior thermal insulation properties as well, with 94% lower thermal conductivity than that of OPC (ISO 8302 method). Mechanical strength assessments reveal that **SunBG$_{90}$** has a compressive strength (35.9 MPa) more than double that required of OPC for residential building foundations (17 MPa). Appropriate additives have also been identified to allow **SunBG$_{90}$** to meet high flame retardance standards (94 V-2 classification, in UL-94 V test) [51]. Collectively, these findings position **SunBG$_{90}$** for significant commercial potential, offering a high-performance, carbon-sequestering alternative to conventional cementitious materials.

Although **SunBG$_{90}$** exhibits significant desirable features, an initial drawback of high free fatty acid feedstocks like BG is that they are not very miscible with molten elemental sulfur, so metal salts or plant oils had to be added as compatibilizers, detracting from the greenness and affordability of the materials [54]. More recent work showed that the high free fatty acids in BG can be chemically modified to improve BG-sulfur miscibility without relying on added metal ions or edible plant oils. A particularly promising route in this vein is the esterification of BG fatty acids with allyl alcohol to form allylated brown grease (**aBG**, a mixture of allyl esters of BG triglycerides) [53]. In addition to being fully miscible with molten sulfur without added compatibilizing agents, the added allyl groups boost the density of reactive C═C bonds for crosslinking. The additional crosslinking yields HSMs that preserve the advantages of BG-derived polymers while improving upcycled mass efficiency and structural homogeneity.

Despite these advances, many HSMs, including those based on BG, often exhibit brittleness or low-impact resistance. Hasell and co-workers recently demonstrated a strategy to enhance toughness in inverse-vulcanized polymers by reinforcing them

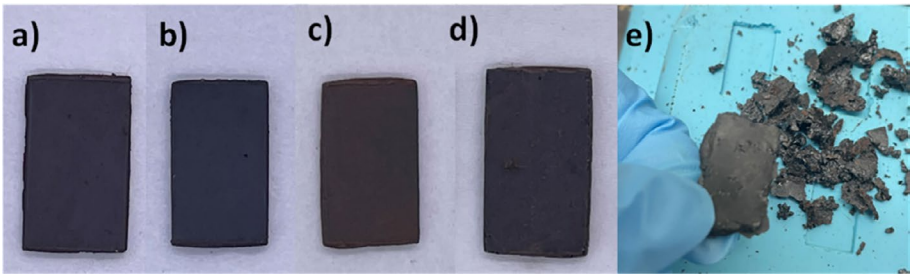

FIGURE 1 | Photos of (a) **aBG$_{90}$**-1.0 wt. % PBD (b) **aBG$_{90}$**-2.0 wt. % PBD, (c) **SunBG$_{90}$**-0.5 wt. % PBD, (d) **SunBG$_{90}$**-1.0 wt. % PBD and (e) **aBG$_{90}$**-3.0 wt. % PBD in rectangular prism form. The brittle nature of non-remeltable **aBG$_{90}$** + 3.0 wt. % PBD is evident from the ease with which it is shattered into powder upon applying moderate force.

with liquid polybutadiene (PBD) [36]. Analogous to high-impact polystyrene, wherein a rubbery phase dissipates strain and prevents catastrophic crack propagation, polybutadiene domains confer improved ductility and resilience to HSMs.

We hypothesized that incorporating polybutadiene into brown grease-based HSMs could provide similar mechanical benefits to BG-sulfur composites (Scheme 1B). Herein, we describe the synthesis, characterization, and thermomechanical property evaluations of polybutadiene-reinforced BG HSMs and evaluate the extent to which the amount of added PBD (0.5–2.0 wt. %) influences the properties of **SunBG$_{90}$** (HSM made from 5 wt. % BG, 5 wt. % sunflower oil, and 90 wt. % sulfur) and **aBG$_{90}$** (HSM made from 90 wt. % sulfur and 10 wt. % **aBG**). This work extended the scope of BG upcycling strategies and adds to efforts to prepare more durable sulfur-rich composites for structural and engineering applications.

2 | Results and Discussion

2.1 | Composite Preparation and Initial Characterization

Hasell's group revealed that the relative proportion of *cis*-1,4, *trans*-1,4, and 1,2-vinylic olefins in PBD had a significant impact on the mechanical properties of the resultant PBD-reinforced HSMs [36]. High *cis*-1,4-content PBD gave the most favorable reinforcement properties and was thus selected for the current study. The high *cis*-1,4 content of the commercial PBD used in this study was confirmed by ^{1}H NMR spectrometry (Figure S1 in the ESI). Samples of **SunBG$_{90}$** and **aBG$_{90}$** to be reinforced were prepared according to literature procedures. PBD was added to molten samples of **SunBG$_{90}$** or **aBG$_{90}$** followed by heating at 180°C for 2 h to yield **SunBG$_{90}$**-x% PBD (x = 0.5 or 1.0 wt. %) and **aBG$_{90}$**-x% PBD (x = 1.0, 2.0, or 3.0 wt. %), respectively.

The resulting materials were black/brown solids, similar to the starting composites **SunBG$_{90}$** or **aBG$_{90}$**. The **SunBG$_{90}$**-x% PBD materials were remeltable solids up to 1% PBD loads; in contrast, **aBG$_{90}$**-x% PBD solids were remeltable up to 2% PBD loads. At 3% material were brittle and easily shattered (Figure 1). Infrared spectral analysis of the materials (Figure S2 in the ESI) showed weak bands attributable to PBD alkene C—H bends after reaction in spectra for all materials, indicating that not all alkene pi bonds underwent crosslinking (spectra are provided in Figure S2); however, formation of S–Callylic bonds is an alternative mechanism for crosslinking noted by Hasell's group that leaves pi bonds intact to form structures like InV-3 (Scheme 1A) [36].

TABLE 1 | Thermal properties of materials.

Materials	T_d[a] (°C)	Char yield (%)[b]	T_m[c] (°C)	$T_{g,DSC}$[d] (°C)	$T_{g,DMA}$[e] (°C)
aBG$_{90}$	223	5	118	NA	−42
aBG$_{90}$-1% PBD	212	6	118	−35	−38
aBG$_{90}$-2% PBD	215	8	118	−36	−45
SunBG$_{90}$	226	9	115	−37	−41
SunBG$_{90}$-0.5% PBD	220	3	119	−35	−36
SunBG$_{90}$-1% PBD	214	7	120	−36	−45

[a]Temperature at which the 5% mass loss was observed.
[b]Amount of material left over after being subjected to high-temperature pyrolysis.
[c]Temperature at the peak maximum of the endothermic melting.
[d]Glass transition temperature obtained from DSC third heating cycle.
[e]Glass transition temperature obtained from DMA storage modulus.

2.2 | Thermal Properties

Analyses of the aBG$_{90}$ and SunBG$_{90}$ materials by thermogravimetric analysis (TGA) with and without added PBD are summarized in Table 1 (full traces provided in Figure S3). All samples displayed thermal stability suitable for structural applications, with decomposition temperatures (T_d) ranging from 212°C to 226°C. The addition of PBD slightly decreased the decomposition onset temperature in most cases, likely due to the lower thermal stability of the polybutadiene domains compared with the sulfur matrix. However, all materials retained thermal robustness well above the typical service temperature of cementitious material used in general construction applications.

Glass transition temperatures (T_g), measured by differential scanning calorimetry (DSC), were observed between −36°C and −37°C for all samples, consistent with the presence of flexible polysulfide domains (Table 1, full traces provided in

Figures S4–S8) [55–57]. Notably, the T_g values did not shift dramatically with PBD incorporation, suggesting that the rubbery PBD segments did not significantly plasticize the matrix but instead acted to reinforce it structurally.

The melting temperature (T_m) of crystalline sulfur remained approximately constant (115°C–120°C). Char yields ranged from 3% to 9%, with higher char retention observed in **SunBG$_{90}$** and **aBG$_{90}$** samples containing greater PBD content, suggesting that the PBD contributes to increased residue during pyrolysis.

2.3 | Mechanical Properties

Mechanical testing (Summarized in Table 2, SI Figures S9–S20) revealed a dramatic improvement in performance upon PBD addition to both **aBG$_{90}$** and **SunBG$_{90}$** matrices (Table 2). To better capture the influence of crosslinking and rubber domain reinforcement, storage modulus values were also evaluated at 25°C, in the rubbery region well above the glass transition. In this regime, network connectivity and long-range molecular architecture play a dominant role in mechanical behavior. For **aBG$_{90}$**, the storage modulus (E') measured by dynamic mechanical analysis (DMA) at 25°C increased from 157 MPa in the unmodified material to 455 MPa with 1% PBD and 700 MPa with 2% PBD. This more than fivefold improvement in stiffness confirms the reinforcing effect of PBD domains. Flexural strength increased progressively from 3.9 MPa (**aBG$_{90}$**) to 5.26 MPa (**aBG$_{90}$**-2% PBD), with concomitant increases in flexural modulus (from 255 MPa to 331 MPa).

For **SunBG$_{90}$**, the mechanical response to PBD addition followed a non-monotonic trend. The storage modulus at 25°C initially decreased from 642 MPa in the baseline **SunBG$_{90}$** to 495 MPa with 0.5% PBD, but then increased to 872 MPa at 1% PBD. This trend may reflect changes in phase structure or dispersion efficiency at low PBD loadings. Interestingly, while stiffness increased significantly, flexural strength plateaued around 5.3–5.4 MPa, slightly lower than the previously reported 7.7 MPa for **SunBG$_{90}$**. This may reflect a trade-off between stiffness and strain-to-failure, where increased rigidity can reduce the material's ability to accommodate localized stress without fracture. Flexural modulus also showed a non-linear trend, peaking at 560 MPa for the 0.5% PBD sample before decreasing slightly at higher PBD content.

TABLE 2 | Mechanical properties of materials.

Materials	Storage modulus (MPa)[a]	Flexural strength (MPa)[b]	Flexural modulus (MPa)[c]
aBG$_{90}$	157	3.9 ± 0.2	255 ± 18
aBG$_{90}$-1% PBD	455	4.4 ± 0.5	272 ± 13
aBG$_{90}$-2% PBD	700	5.26 ± 0.05	331 ± 65
SunBG$_{90}$[d]	642	7.7 ± 0.3	460
SunBG$_{90}$-0.5% PBD	495	5.4 ± 0.2	560 ± 63
SunBG$_{90}$-1% PBD	872	5.3 ± 0.2	337 ± 62

[a]Maximum value, occurring at 25°C.
[b]Measured in triplicate in single cantilever mode, with standard deviations.
[c]Measured in triplicate in single cantilever mode, calculated from the initial linear regime, with standard deviations.
[d]Values reported previously.

These observations reveal that **SunBG$_{90}$** requires less PBD to achieve mechanical reinforcement than **aBG$_{90}$**. The greater initial crosslink density and compositional complexity of **SunBG$_{90}$**—due to its incorporation of both brown grease and sunflower oil—may facilitate more effective PBD integration at lower loadings. In contrast, **aBG$_{90}$**, which relies on a single bio-derived esterified feedstock with a preponderance of allyl olefins rather than the all-*cis* alkenes in **SunBG$_{90}$**-derived materials, requires higher PBD content to reach comparable performance.

The data show that PBD reinforcement leads to a near-linear increase in storage modulus for both **aBG$_{90}$** and **SunBG$_{90}$** systems, while the trends in flexural strength and flexural modulus are more complex and non-linear, particularly in the case of **SunBG$_{90}$**. This contrast can be rationalized by considering how different mechanical properties respond to molecular-scale structure and phase behavior within these sulfur-rich polymer networks.

The storage modulus primarily reflects the elastic stiffness of the polymer network under small, oscillatory deformations, typically in the glassy regime at low temperatures (−60°C). At these temperatures, below the T_g, molecular motions are highly restricted, and the material's response is dominated by network connectivity and density of physical or chemical crosslinks [58–60].

The linear increase in E' with increasing PBD content suggests that PBD chains are progressively incorporated into the crosslinked network by sulfur–alkene reactions that form new crosslinks between PBD and the sulfur matrix. With each incremental addition of PBD, more flexible rubbery segments are included in the rigid sulfur-rich network, increasing segmental interactions and limiting chain mobility. This uniformly enhances the stiffness measured by DMA, especially at low temperatures where energy dissipation mechanisms are minimized.

The nonlinear influence of PBD reinforcement on flexural strength and flexural modulus reflects the material's ability to resist larger-scale bending and deformation under load near room temperature (above the T_g). These properties depend not only on network stiffness but also on stress distribution, crack initiation, and energy dissipation pathways, all of which are influenced by microphase separation, local domain structure, and fracture mechanics. In this regime, low PBD loadings (e.g., 0.5%–1%) are expected to improve stress dissipation by introducing rubbery domains that act as energy-absorbing zones, analogous to the role of rubber particles in toughened thermosets [58–60]. However, excessive PBD content may lead to local heterogeneities, decreased interfacial adhesion between phases, or microphase separation. These features can act as stress concentrators that hinder further improvements in flexural performance or even reduce it, as possibly observed in

SunBG$_{90}$ where the flexural modulus decreases from 560 MPa (0.5% PBD) to 337 MPa (1% PBD).

The data for PBD-reinforced composites delineated herein align with and extend the reinforcement trends reported by Hasell and coworkers. In Hasell's work, PBD was incorporated at relatively high loadings (10–30 wt. %) into sulfur-DIB composites (DIB = 1,3-bis(2-isopropenyl)benzene) to overcome the intrinsic brittleness of these high-sulfur materials. They reported flexural strengths increasing from ~4 MPa (for S-DIB) to ~30 MPa with 30 wt. % PBD and impact resistance that more than doubled. However, such high PBD loadings often reduced char yield and introduced phase separation challenges, particularly with high-vinyl-content PBDs.

In contrast, the current study shows that substantially lower PBD loadings (0.5–3.0 wt. %) are sufficient to effect significant mechanical reinforcement in brown grease-derived sulfur polymers, particularly when starting from a matrix like **SunBG$_{90}$** that already exhibits high crosslink density and phase homogeneity. For example, 1 wt. % PBD raised the storage modulus of **SunBG$_{90}$** from ~460 MPa to over 1500 MPa—comparable to the reinforcement seen in Hasell's highest-loading materials but achieved with far less PBD additive. Similarly, in **aBG$_{90}$**, the storage modulus increased from 295 MPa to 1533 MPa with just 2 wt. % PBD, a more than fivefold increase.

2.4 | Reprocessability

To investigate the reprocessability of the material, which is a key advantage of high sulfur-based composites, we selected **aBG$_{90}$**-2% PBD formulation due to its superior mechanical performance compared with other tested materials. Among the **aBG$_{90}$** and **SunBG$_{90}$** series, **aBG$_{90}$**-2% PBD exhibited the highest storage modulus (700 MPa) and a high flexural strength (5.26 ± 0.05 MPa), indicating a stiffer and more robust material under both dynamic and static loading conditions. Its flexural modulus (331 ± 65 MPa) was also higher than that of unfilled **aBG$_{90}$** and **aBG$_{90}$**-1% PBD. While **SunBG$_{90}$**-1% PBD showed a higher storage modulus (872 MPa), with similar flexural strength (5.3 ± 0.2 MPa), it presented a larger variability in modulus.

The unprocessed material exhibited a storage modulus of 700 MPa. Interestingly, the first remelting resulted in an increase in stiffness (828 MPa), likely due to post-curing or improved filler dispersion. A general decline followed across subsequent cycles, with values ranging from 580 to 635 MPa between cycles 2 and 7, corresponding to 82.9%–90.6% retention of the original modulus. After the eighth cycle, retention dropped to 54.7%; but a notable rebound was observed at the ninth cycle (92.4%, 647 MPa), followed by 69.6% retention at the tenth (487 MPa), as shown in Figure S22. Despite these fluctuations, the material consistently preserved a substantial fraction of its stiffness across multiple remelting events. This behavior is consistent with early findings by Thiounn et al. [61], which likewise demonstrated that high sulfur-content materials retained 80–100% of their original storage modulus over seven reprocessing cycles, highlighting their amenability to thermal recyclability. These results confirm that the composite in this study is suitable for repeated thermal reuse, reinforcing its promise for sustainable materials applications.

3 | Conclusions

This work demonstrates that low loadings (0.5–2 wt. %) of high cis-1,4 liquid polybutadiene (PBD) can significantly reinforce brown grease-derived sulfur polymers, including both **SunBG$_{90}$** and allylated brown grease-based **aBG$_{90}$**. Incorporation of PBD resulted in substantial improvements in storage modulus, with a near-linear increase observed as a function of PBD content. In **aBG$_{90}$**, stiffness increased more than fivefold with only 2 wt. % PBD, while **SunBG$_{90}$** achieved similar reinforcement at just 1 wt. %, reflecting the more crosslinked and structurally integrated nature of the **SunBG$_{90}$** matrix.

Flexural properties, in contrast, displayed non-linear trends with PBD loading, suggesting complex interplay between matrix compatibility, microphase structure, and failure mechanisms. These observations highlight the distinct molecular and morphological factors that govern different mechanical responses in high-sulfur materials.

Thermal analyses confirmed that PBD-modified composites retained high thermal stability (T_d > 210°C) and consistent glass transition behavior, supporting their suitability for structural applications under thermal stress. Compared with previous studies requiring higher PBD loadings, the low additive thresholds reported here offer a more sustainable pathway to mechanically robust, bio-derived sulfur polymers. These findings expand the design space for durable, recyclable materials from waste-derived inputs and suggest future opportunities in lightweight construction, coatings, and thermal insulation applications.

Taken together, these findings suggest that bio-derived, sulfur-rich composites like **aBG$_{90}$** and **SunBG$_{90}$** can be efficiently reinforced with PBD at low loadings, yielding materials with stiffness and strength approaching those of high-impact engineering polymers, while maintaining processability and low-cost, renewable content. The reduced need for PBD also improves sustainability by minimizing reliance on petrochemical inputs. This represents a significant advance in the design of tough, recyclable sulfur materials suitable for demanding structural applications.

4 | Experimental Section

4.1 | Chemicals and Materials

Sulfur powder was purchased from Dugas Diesel. Allyl bromide (99% stabilized with 300–1000 ppm propylene oxide) was purchased from Alfa Aesar. Brown grease (supplied by the Animal Coproducts Research and Education Center). Acetone was obtained from Fisher. Sunflower oil was obtained from Maple Holistics. Polybutadiene was purchased from Sigma-Aldrich. The chemicals were used without further purification unless otherwise specified. The composites **aBG$_{90}$** and **SunBG$_{90}$** were prepared as previously reported [47, 53].

4.2 | Synthesis of Composites

CAUTION: Heating elemental sulfur with organics can consequently result in H_2S or other gas formation. Such gases can be

corrosive, foul-smelling, and toxic. Temperature must be cautiously controlled in order to prevent thermal spikes, contributing to the potential for H2S or other gas evolution. Rapid stirring, shortened heating times, and very slow addition of reagents can help avoid unforeseen temperature spikes.

4.2.1 | General Synthesis of PBD Reinforced aBG_{90} and $SunBG_{90}$

The composite to be modified (**aBG_{90}** or **$SunBG_{90}$**) was weighed and placed in a scintillation vial. Afterward, the vial containing the composite and a stir bar was placed in an oil bath at 180°C. Once melted, mechanical stirring was started, and the desired amount of polybutadiene (0.5–3.0 wt. %) was added to the melted composite. The reaction was carried out for 2 h. The brown/black solid product was allowed to cool to ambient temperature.

4.3 | Instrumentation

Shimadzu IR Affinity-1S instrument with an ATR attachment operating over 400–4000 cm^{-1} at ambient temperature was used to obtain Fourier transform infrared spectra.

The proton NMR spectra were acquired using a Bruker NEO-300 MHz spectrometer at room temperature. TopSpin 3.7.0 software was used to process the data.

Thermogravimetric analysis (TGA) data were recorded (Mettler Toledo TGA 2 STARe System, TA Instruments, New Castle, DE, USA) across the temperature range 20°C–800°C at a heating rate of 10°C·min^{-1} under a flow of N_2 (100 mL·min^{-1}).

Differential scanning calorimetry (DSC) data were acquired using a Mettler Toledo DSC 3 STARe System from −60°C to 140°C, with a heating rate of 10°C min^{-1} under N_2 (50 mL min^{-1}). Each DSC measurement was carried out over three heat-cool cycles, and data were reported for the third cycle.

Flexural strength testing and Dynamic Mechanical Analysis (DMA) were performed using a Mettler Toledo DMA 1 STARe System in single cantilever mode. For flexural strength, the temperature was fixed at 25°C. For DMA, the frequency and amplitude were set at 1 Hz and 5 μm, respectively. DMA samples were cast from silicone resin molds (Smooth-On Mold StarTM 30 platinum silicon rubber). The sample dimensions were 1.3 × 10.8 × 5.0 mm. The clamping force was 1 cN m for both analyses. For DMA, the temperature ranged from −60°C to 80°C. The samples were tested in triplicates, and the results were averaged.

Acknowledgments

Funding for this project from the National Science Foundation (CHE-2203669 to R.C.S.) and a seed grant from the South Carolina Department of Agriculture ACRE program (to R.C.S. and A.D.S.) is gratefully acknowledged.

Conflicts of Interest

The authors declare no conflicts of interest.

References

1. W. J. Chung, J. J. Griebel, E. T. Kim, et al., "The Use of Elemental Sulfur as an Alternative Feedstock for Polymeric Materials," *Nature Chemistry* 5 (2013): 518–524.

2. J. Bao, K. P. Martin, E. Cho, et al., "On the Mechanism of the Inverse Vulcanization of Elemental Sulfur: Structural Characterization of Poly(Sulfur-Random-(1,3-Diisopropenylbenzene))," *Journal of the American Chemical Society* 145 (2023): 12386–12397.

3. J. Molineux, T. Lee, K. J. Kim, et al., "Fabrication of Plastic Optics From Chalcogenide Hybrid Inorganic/Organic Polymers for Infrared Thermal Imaging," *Advanced Optical Materials* 12 (2024): 2301971.

4. Z. Song, W. Jiang, B. Li, et al., "Advanced Polymers in Cathodes and Electrolytes for Lithium–Sulfur Batteries: Progress and Prospects," *Small* 20 (2024): 2308550.

5. S. Ren, P. Sang, W. Guo, and Y. Fu, "Organosulfur Polymer-Based Cathode Materials for Rechargeable Batteries," *Polymer Chemistry* 13 (2022): 5676–5690.

6. C. V. Lopez, C. P. Maladeniya, and R. C. Smith, "Lithium-Sulfur Batteries: Advances and Trends," *Electrochemistry* 1 (2020): 226–259.

7. A. Nayeem, M. F. Ali, and J. H. Shariffuddin, "The Recent Development of Inverse Vulcanized Polysulfide as an Alternative Adsorbent for Heavy Metal Removal in Wastewater," *Environmental Research* 216 (2023): 114306.

8. F. G. Müller, L. S. Lisboa, and J. M. Chalker, "Inverse Vulcanized Polymers for Sustainable Metal Remediation," *Advanced Sustainable Systems* 7 (2023): 2300010.

9. Z. Huang, Y. Deng, and D.-H. Qu, "Adding Value Into Elementary Sulfur for Sustainable Materials," *Chemistry – A European Journal* 31 (2025): e202500125.

10. K. B. Sayer, V. L. Miller, Z. Merrill, A. E. Davis, and C. L. Jenkins, "Allyl Sulfides in Garlic Oil Initiate the Formation of Renewable Adhesives," *Polymer Chemistry* 14 (2023): 3091–3098.

11. C. Herrera, K. J. Ysinga, and C. L. Jenkins, "Polysulfides Synthesized From Renewable Garlic Components and Repurposed Sulfur Form Environmentally Friendly Adhesives," *ACS Applied Materials & Interfaces* 11 (2019): 35312–35318.

12. A. E. Davis, K. B. Sayer, and C. L. Jenkins, "A Comparison of Adhesive Polysulfides Initiated by Garlic Essential Oil and Elemental Sulfur to Create Recyclable Adhesives," *Polymer Chemistry* 13 (2022): 4634–4640.

13. P. Yan, W. Zhao, S. J. Tonkin, J. M. Chalker, T. L. Schiller, and T. Hasell, "Stretchable and Durable Inverse Vulcanized Polymers With Chemical and Thermal Recycling," *Chemistry of Materials* 34 (2022): 1167–1178.

14. J. A. Smith, S. J. Green, S. Petcher, et al., "Crosslinker Copolymerization for Property Control in Inverse Vulcanization," *Chemistry - A European Journal* 25 (2019): 10433–10440.

15. P. Yan, W. Zhao, B. Zhang, et al., "Angewandte Chemie," *International Edition* 59 (2020): 13371–13378.

16. V. Hanna, P. Yan, S. Petcher, and T. Hasell, "Incorporation of Fillers to Modify the Mechanical Performance of Inverse Vulcanised Polymers," *Polymer Chemistry* 13 (2022): 3930–3937.

17. R. F. Naylor, "Modern Views on the Chemistry of Vulcanization Changes. II. Role of Hydrogen Sulfide," *Journal of Polymer Science* 1 (1946): 305–311.

18. M. Akiba and A. S. Hashim, "Progress in Polymer Science," 22 (1997): 475–521.

19. H. Shen, B. Zheng, and H. Zhang, "A Decade Development of Inverse Vulcanization Towards Green and Sustainable Practices," *Polymer Reviews* 64 (2024): 1211–1266.

20. K.-S. Kang, K. A. Iyer, and J. Pyun, "On the Fundamental Polymer Chemistry of Inverse Vulcanization for Statistical and Segmented

Copolymers From Elemental Sulfur," *Chemistry - A European Journal* 28 (2022): e202200115.

21. A. S. M. Ghumman, M. M. Nasef, M. R. Shamsuddin, and A. Abbasi, "Evaluation of Properties of Sulfur-Based Polymers Obtained by Inverse Vulcanization: Techniques and Challenges," *Polymers and Polymer Composites* 29 (2020): 1333–1352.

22. L. J. Dodd, "Inverse Vulcanisation: A New Starter's Guide to an Emerging Field," *RSC Applied Polymers* 3 (2025): 10–42.

23. A. Demirbas, H. Alidrisi, and M. A. Balubaid, "API Gravity, Sulfur Content, and Desulfurization of Crude Oil," *Petroleum Science and Technology* 33 (2015): 93–101.

24. J. Wolfs, I. Ribca, M. A. R. Meier, and M. Johansson, "Polythionourethane Thermoset Synthesis via Activation of Elemental Sulfur in an Efficient Multicomponent Reaction Approach," *ACS Sustainable Chemistry & Engineering* 11 (2023): 3952–3962.

25. P. Conen, R. Nickisch, and M. A. R. Meier, "Synthesis of Highly Substituted Alkenes by Sulfur-Mediated Olefination of N-Tosylhydrazones," *Communications Chemistry* 6 (2023): 255.

26. M. K. Lauer, A. G. Tennyson, and R. C. Smith, "Inverse Vulcanization of Octenyl Succinate-Modified Corn Starch as a Route to Biopolymer–Sulfur Composites," *Materials Advances* 2 (2021): 2391–2397.

27. M. K. Lauer, A. G. Tennyson, and R. C. Smith, "Green Synthesis of Thermoplastic Composites From a Terpenoid-Cellulose Ester," *ACS Applied Polymer Materials* 2 (2020): 3761–3765.

28. M. K. Lauer, M. S. Karunarathna, A. G. Tennyson, and R. C. Smith, "Robust, Remeltable and Remarkably Simple to Prepare Biomass–Sulfur Composites," *Materials Advances* 1 (2020): 2271–2278.

29. M. K. Lauer, M. S. Karunarathna, A. G. Tennyson, and R. C. Smith, "Recyclable, Sustainable, and Stronger Than Portland Cement: A Composite From Unseparated Biomass and Fossil Fuel Waste," *Materials Advances* 1 (2020): 590–594.

30. M. S. Karunarathna, A. G. Tennyson, and R. C. Smith, "Facile New Approach to High Sulfur-Content Materials and Preparation of Sulfur–Lignin Copolymers," *Journal of Materials Chemistry A: Materials for Energy and Sustainability* 8 (2020): 548–553.

31. M. S. Karunarathna, M. K. Lauer, A. G. Tennyson, and R. C. Smith, "Copolymerization of an Aryl Halide and Elemental Sulfur as a Route to High Sulfur Content Materials," *Polymer Chemistry* 11 (2020): 1621–1628.

32. B. Zhang, S. Petcher, H. Gao, et al., "Magnetic Sulfur-Doped Carbons for Mercury Adsorption," *Journal of Colloid and Interface Science* 603 (2021): 728–737.

33. B. Zhang, H. Gao, P. Yan, S. Petcher, and T. Hasell, "Inverse Vulcanization Below the Melting Point of Sulfur," *Materials Chemistry Frontiers* 4 (2020): 669–675.

34. P. Yan, W. Zhao, F. McBride, et al., "Mechanochemical Synthesis of Inverse Vulcanized Polymers," *Nature Communications* 13 (2022): 4824.

35. S. J. Tonkin, C. T. Gibson, J. A. Campbell, et al., "Chemically Induced Repair, Adhesion, and Recycling of Polymers Made by Inverse Vulcanization," *Chemical Science* 11 (2020): 5537–5546.

36. V. Hanna, M. Graysmark, H. Willcock, and T. Hasell, "Liquid Polybutadiene Reinforced Inverse Vulcanised Polymers," *Journal of Materials Chemistry A* 12 (2024): 1211–1217.

37. J. C. Bear, J. D. McGettrick, I. P. Parkin, C. W. Dunnill, and T. Hasell, "Porous Carbons From Inverse Vulcanised Polymers," *Microporous and Mesoporous Materials* 232 (2016): 189–195.

38. M. J. H. Worthington, R. L. Kucera, I. S. Albuquerque, et al., "Laying Waste to Mercury: Inexpensive Sorbents Made From Sulfur and Recycled Cooking Oils," *Chemistry - A European Journal* 23 (2017): 16219–16230.

39. F. Stojcevski, M. K. Stanfield, D. J. Hayne, et al., "Inverse Vulcanisation of Canola Oil as a Route to Recyclable Chopped Carbon Fibre Composites," *Sustainable Materials and Technologies* 32 (2022): e00400.

40. J. M. M. Pople, T. P. Nicholls, L. N. Pham, et al., "Electrochemical Synthesis of Poly(Trisulfides)," *Journal of the American Chemical Society* 145 (2023): 11798–11810.

41. J. M. Phillips, M. Ahamed, X. Duan, et al., "Chemoselective and Continuous Flow Hydrogenations in Thin Films Using a Palladium Nanoparticle Catalyst Embedded in Cellulose Paper," *ACS Applied Bio Materials* 2 (2019): 488–494.

42. N. A. Lundquist, Y. Yin, M. Mann, et al., "Magnetic Responsive Composites Made From a Sulfur-Rich Polymer," *Polymer Chemistry* 13 (2022): 5659–5665.

43. N. A. Lundquist, A. D. Tikoalu, M. J. H. Worthington, et al., "Reactive Compression Molding Post-Inverse Vulcanization: A Method to Assemble, Recycle, and Repurpose Sulfur Polymers and Composites," *Chemistry - A European Journal* 26 (2020): 10035–10044.

44. L. J. Esdaile and J. M. Chalker, "The Mercury Problem in Artisanal and Small-Scale Gold Mining," *Chemistry - A European Journal* 24 (2018): 6905–6916.

45. A. D. Smith, R. C. Smith, and A. G. Tennyson, "Sulfur-Containing Polymers Prepared From Fatty Acid-Derived Monomers: Application of Atom-Economical Thiol-Ene/Thiol-Yne Click Reactions and Inverse Vulcanization Strategies," *Sustainable Chemistry* 1 (2020): 209–237.

46. C. P. Maladeniya, M. S. Karunarathna, M. K. Lauer, C. V. Lopez, T. Thiounn, and R. C. Smith, "A Role for Terpenoid Cyclization in the Atom Economical Polymerization of Terpenoids With Sulfur to Yield Durable Composites," *Materials Advances* 1 (2020): 1665–1674.

47. C. V. Lopez, A. D. Smith, and R. C. Smith, "High Strength Composites From Low-Value Animal Coproducts and Industrial Waste Sulfur," *RSC Advances* 12 (2022): 1535–1542.

48. B. G. S. Guinati, P. Y. Sauceda Oloño, N. L. Kapuge Dona, et al., "Upcycling Mixed-Material Waste With Elemental Sulfur: Applications to Plant Oil, Unseparated Biomass, and Raw Post-Consumer Food Waste," *RSC Sustainability* 2 (2024): 1819–1827.

49. S. K. Wijeyatunga, P. Y. Sauceda-Oloño, N. L. Kapuge Dona, et al., "Static and Dynamic Assessments of a Sulfur-Triglyceride Composite for Antimicrobial Surface Applications," *Molecules* 30 (2025): 1614, https://doi.org/10.3390/molecules30071614.

50. P. Y. Sauceda-Oloño, C. V. Lopez, B. K. Patel, A. D. Smith, and R. C. Smith, "Influence of Thermal and Chemical Stresses on Thermal Properties, Crystal Morphology, and Mechanical Strength Development of a Sulfur Polymer Composite," *Macromol* 4 (2024): 240–252, https://doi.org/10.3390/macromol4020013.

51. P. Y. Sauceda-Oloño, B. G. S. Guinati, A. D. Smith, and R. C. Smith, "Influence of Additives on Flame-Retardant, Thermal, and Mechanical Properties of a Sulfur–Triglyceride Polymer Composite," *Journal Of Composites Science* 8 (2024): 080304, https://doi.org/10.3390/jcs8080304.

52. P. Y. Sauceda-Olono, A. C. Borbon-Almada, M. Gaxiola, A. D. Smith, A. G. Tennyson, and R. C. Smith, "Thermal and Mechanical Properties of Recyclable Composites Prepared from Bio-Olefins and Industrial Waste," *Journal Of Composites Science* 7 (2023): 248–259.

53. B. G. S. Guinati, S. K. Wijeyatunga, A. D. Smith, A. G. Tennyson, and R. C. Smith, "Brown Grease Esterification: A Design Strategy to Modulate Homogeneity, Cross-Linking, and Upcycled Mass Economy in High Sulfur-Content Materials," *Journal of Polymer Science* 63 (2025): 2651–2661, https://doi.org/10.1002/pol.20250206.

54. A. D. Smith, T. Thiounn, E. W. Lyles, E. K. Kibler, R. C. Smith, and A. G. Tennyson, "Journal of Polymer Science," *Part A: Polymer Chemistry* 57 (2019): 1704–1710.

55. B. Meyer, "Solid Allotropes of Sulfur," *Chemical Reviews* 64 (1964): 429–451.

56. C. P. Maladeniya and R. C. Smith, "Influence of Component Ratio on Thermal and Mechanical Properties of Terpenoid-Sulfur Composites," *Journal Of Composites Science* 5 (2021): 257.

57. M. S. Karunarathna, C. P. Maladeniya, M. K. Lauer, A. G. Tennyson, and R. C. Smith, "Durable Composites by Vulcanization of Oleyl-Esterified Lignin," *RSC Advances* 13 (2023): 3234–3240.

58. I. M. Ward, *Mechanical Properties of Solid Polymers* (Wiley, 2012).

59. H. F. Brinson and L. C. Brinson, *Polymer Engineering Science and Viscoelasticity: An Introduction* (Springer, 2015).

60. N. E. Dowling, *Mechanical Behavior of Materials: Engineering Methods for Deformation, Fracture, and Fatigue* (Pearson, 2012).

61. T. Thiounn, M. K. Lauer, M. S. Bedford, R. C. Smith, and A. G. Tennyson, "Thermally-Healable Network Solids of Sulfur-Crosslinked Poly(4-Allyloxystyrene)," *RSC Advances* 8 (2018): 39074–39082.

Supporting Information

Additional supporting information can be found online in the Supporting Information section. **Data S1:** Supporting Information.